

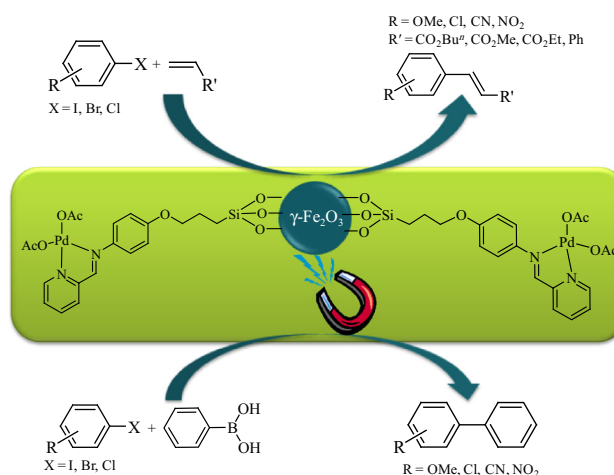
Palladium-Schiff Base Complex Immobilized Covalently on Magnetic Nanoparticles as an Efficient and Recyclable Catalyst for Heck and Suzuki Cross-Coupling Reactions

Sara Sobhani¹ · Zahra Mesbah Falatoni¹ · Solmaz Asadi¹ · Moones Honarmand²

Received: 25 August 2015 / Accepted: 27 September 2015
© Springer Science+Business Media New York 2015

Abstract A new palladium-Schiff base complex immobilized covalently on magnetic nanoparticles (Pd-imino-Py- γ -Fe₂O₃) was synthesized via the reaction of chloro-functionalized γ -Fe₂O₃ with iminopyridine followed by the reaction with palladium acetate. Characterization of Pd-imino-Py- γ -Fe₂O₃ was carried out by various techniques such as XRD, SEM, TEM, FT-IR, TGA, ICP, XPS, VSM and elemental analysis. Pd-imino-Py- γ -Fe₂O₃ was successfully applied as a magnetically recyclable heterogeneous catalyst in Heck and Suzuki cross-coupling reactions of various aryl halides (iodide, bromides and chlorides as challenging substrates) with olefins and phenylboronic acid, respectively. The synthesized catalyst was separated easily by using an external magnet and recycled eight runs without appreciable loss of its catalytic activity and leaching of the significant quantity of Pd.

Graphical Abstract



Keywords Palladium · Magnetic nanoparticles · Heterogeneous catalyst · Heck and Suzuki reactions

1 Introduction

Heck and Suzuki cross-coupling reactions are the most straightforward and powerful transformations for the construction of carbon-carbon bonds which can lead to important substituted olefins and biphenyls. These products play a significant role in medicinal as well as structural chemistry and agriculture. They are used as versatile building blocks for the synthesis of many organic intermediates in material sciences, pharmaceuticals and herbicides [1–4]. Heck and Suzuki cross-coupling reactions have been commonly carried out by using homogeneous palladium catalysts in the presence of phosphine [1, 5, 6],

✉ Sara Sobhani
sobhanisara@yahoo.com; ssobhani@birjand.ac.ir

¹ Department of Chemistry, College of Sciences, University of Birjand, Birjand, Iran

² Department of Chemical Engineering, Faculty of Mining, Chemical and Material Engineering, Birjand University of Technology, Birjand, Iran

imidazole [7], pyridine [8], N-heterocyclic carbenes [9], dibenzylideneacetone (dba) [10], palladacycles [11], thiols [12], porphyrins [13], phthalocyanines [14], bidentate [15] and pincer [16] ligands. They suffer from some drawbacks such as requiring large amount of the catalyst, product contamination, and difficulty in catalyst separation from the reaction mixture and recycling which is a serious problem in the pharmaceutical industry. Considering this intrinsic limitation of homogeneous Pd (expensive metal) catalysts, in addition to environmental and economical concerns, many attempts have been directed toward the development of new strategies to immobilize the homogeneous Pd catalysts onto various solid supports in the form of either metal complexes (by covalent anchoring) or metal nanoparticles (by adsorption) [17]. In heterogenization of Pd catalysts, surface covalent anchoring of Pd complexes is preferred over simple Pd adsorption as it is robust enough to withstand the reaction conditions and the catalyst can be reused several times without significant leaching during the reaction workup.

Among various solid supports used for the heterogenization of Pd catalysts, magnetic nanoparticles (MNPs) have emerged as one of the most useful solid materials [18–23]. The main advantage of MNPs is their simple separation from the reaction mixture by using an external magnet, without any need for filtration or centrifugation. Also, most magnetic-supported catalysts can be reused many times while keeping their initial activity. Moreover, the outstanding dispersion of supported catalysts on MNPs in different solvents is additional benefit, as this makes the active sites of the catalyst more accessible to the reactants. The presence of supported catalysts on the surface of MNPs solves the diffusion limitation problems, which are often observed for supported catalysts for example in microporous or mesoporous matrices [24].

Schiff bases are an important class of organic ligands in coordination chemistry and have been extensively used as metal Schiff base complexes to catalyze organic reactions due to the advantages such as their cost-effective, ease of synthesis, availability and thermal and chemical stability [25]. However, the use of metal Schiff base complexes as catalyst in homogeneous solution suffers from deactivation because of formation of μ -oxo and dimeric peroxo- species, which have been demonstrated to be inactive in various reactions [26, 27]. Moreover, difficulties in separation and reusability of homogeneous metal (particularly expensive metals) Schiff base complexes have limited the applications of these catalysts. For overcoming the aforementioned drawbacks, metal Schiff base complexes can be immobilized on suitable solid supports.

On continuation of our research interest in developing new heterogeneous catalysts [28–41], herein, we have synthesized a new palladium-Schiff base complex

immobilized covalently on γ -Fe₂O₃ (Pd-imino-Py- γ -Fe₂O₃) and used it as a magnetically recyclable heterogeneous palladium catalyst in Heck and Suzuki cross-coupling reactions.

2 Experimental

2.1 General Information

Chemicals were purchased from Merck Chemical Company. NMR spectra were recorded on a Bruker Avance DPX-400 using deuterated CDCl₃ as solvent and TMS as internal standard. The purity of the products and the progress of the reactions were accomplished by TLC on silica-gel polygram SILG/UV254 plates. TEM analysis was performed using TEM microscope (Philips CM30). FT-IR spectra were recorded on a Shimadzu Fourier Transform Infrared Spectrophotometer (FT-IR-8300). Thermo gravimetric analysis (TGA) was performed using a Shimadzu thermo gravimetric analyzer (TG-50). Elemental analysis was carried out on a Costech 4010 CHN elemental analyzer. The morphology of the products was determined by using Hitachi Japan, model s4160 Scanning Electron Microscopy (SEM) at accelerating voltage of 15 kV. Power X-ray diffraction (XRD) was performed on a Bruker D8-advance X-ray diffractometer with Cu K α ($\lambda = 0.154$ nm) radiation. This system was equipped with a concentric hemispherical (CHA) electron energy analyzer (Specs model EA10 plus) suitable for X-ray photoelectron spectroscopy (XPS). The content of Pd in the catalyst was determined by OPTIMA 7300DV ICP analyzer. Room temperature magnetization isotherms were obtained using a vibrating sample magnetometer (VSM, Lake Shore 7400).

2.2 Synthesis of Iminopyridine

Pyridine-2-carbaldehyde (0.5 g) was added to a magnetically stirring mixture of 4-aminophenol (0.5 g) in MeOH (10 mL). After refluxing for 3 h, the mixture was cooled to room temperature. The resulting yellow crystals (iminopyridine ligand) was separated by filtration, washed with MeOH (3 \times 10 mL) and dried under vacuum.

2.3 Synthesis of Schiff Base Immobilized on γ -Fe₂O₃ (Imino-Py- γ -Fe₂O₃)

A solution of chloro-functionalized γ -Fe₂O₃ [34] (1.7 g) in DMF (10 mL) was added dropwise to a stirring solution of iminopyridine (0.15 g) and NaH (0.005 g) in DMF (5 mL), under Ar atmosphere at 80 °C within 1 h. The reaction mixture was stirred at 80 °C for another

24 h. The resulting Schiff base immobilized on γ -Fe₂O₃ was separated by an external magnet, washed with acetone (3 × 10 mL) and dried under vacuum. The loading amount of Schiff base was 0.28 mmol g⁻¹ catalyst based on elemental analysis.

2.4 Synthesis of Palladium-Schiff Base Complex Immobilized on γ -Fe₂O₃ (Pd-Imino-Py- γ -Fe₂O₃)

The synthesized Schiff base immobilized on γ -Fe₂O₃ (1.7 g) was added to a solution of palladium acetate (0.12 g) in dry acetone (5 mL). The reaction mixture was stirred at room temperature for 24 h. The solid was separated by an external magnet, and washed with acetone (3 × 10 mL) and dried under vacuum to afford Pd-imino-Py- γ -Fe₂O₃.

2.5 General Procedure for Heck Coupling Reaction

A mixture of aryl halide (1 mmol), olefin (1.5 mmol), Et₃N (2 mmol) and Pd-imino-Py- γ -Fe₂O₃ (0.25 mol%, 0.009 g) was stirred at 100 °C in DMF (2 mL) for an appropriate time (Table 2). The catalyst was separated by an external magnet, washed with EtOH, dried and reused for a consecutive run under the same reaction conditions. Evaporation of the solvent of the filtrate under reduced pressure gave the crude products. The pure products were isolated by chromatography on silica gel eluted with *n*-hexane:EtOAc (50:1).

2.5.1 (*E*)-*n*-Butyl Cinnamate (**1a**)

¹H NMR (400 MHz, CDCl₃): δ 0.88 (t, 3H, ³J = 7.6 Hz), 1.34–1.36 (m, 2H), 1.59–1.62 (m, 2H), 4.13 (t, 2H, ³J = 6.8 Hz), 6.36 (d, 1H, ³J = 16.0 Hz), 7.29–7.30 (m, 3H), 7.43–7.45 (m, 2H), 7.60 (d, 1H, ³J = 16.4 Hz); ¹³C NMR (100 MHz, CDCl₃): δ 13.7, 19.2, 30.8, 64.3, 118.2, 128.0, 128.8, 130.1, 134.4, 144.4, 166.8.

2.5.2 (*E*)-Methyl Cinnamate (**1b**)

¹H NMR (400 MHz, CDCl₃): δ 3.74 (s, 3H), 6.38 (d, 1H, ³J = 16.4 Hz), 7.31–7.33 (m, 3H), 7.45–7.47 (m, 2H), 7.63 (d, 1H, ³J = 16.4 Hz); ¹³C NMR (100 MHz, CDCl₃): δ 51.6, 117.7, 128.1, 128.9, 130.3, 134.3, 144.8, 167.3.

2.5.3 (*E*)-Methyl 2-Methyl-3-phenylacrylate (**1c**)

¹H NMR (400 MHz, CDCl₃): δ 2.15 (s, 3H), 3.83 (s, 3H), 7.21–7.41 (m, 5H), 7.92 (d, 1H, ³J = 16.0 Hz); ¹³C NMR

(100 MHz, CDCl₃): δ 14.1, 52.0, 127.9, 129.6, 135.8, 138.9, 169.1.

2.5.4 (*E*)-Ethyl cinnamate (**1d**)

¹H NMR (400 MHz, CDCl₃): δ 1.43 (t, 3H, ³J = 8.0 Hz), 4.19 (q, 2H, ³J = 8.0 Hz), 6.35 (d, 1H, ³J = 16 Hz), 7.27–7.28 (m, 3H), 7.41–7.42 (m, 2H), 7.63 (d, 1H, ³J = 16.0 Hz); ¹³C NMR (100 MHz, CDCl₃): δ 14.2, 60.0, 118.2, 127.9, 128.7, 130.1, 134.3, 144.3, 166.6.

2.5.5 (*E*)-1,2-Diphenylethene (**1e**)

¹H NMR (400 MHz, CDCl₃): δ 7.18 (s, 2H), 7.33 (t, 2H, ³J = 6.8 Hz), 7.42 (t, 4H, ³J = 7.0 Hz), 7.58 (d, 4H, ³J = 7.2 Hz); ¹³C NMR (100 MHz, CDCl₃): δ 126.7, 127.8, 128.8, 137.4.

2.5.6 (*E*)-*n*-Butyl 3-(4-methoxyphenyl)acrylate (**1f**)

¹H NMR (400 MHz, CDCl₃): δ 0.91 (t, 3H, ³J = 7.0 Hz), 1.35–1.40 (m, 2H), 1.60–1.62 (m, 2H), 3.72 (s, 3H), 4.13 (m, 2H, ³J = 7.0 Hz), 6.24 (d, 1H, ³J = 16.0 Hz), 6.81 (d, 3H, ³J = 4.8 Hz), 7.39 (d, 3H, ³J = 4.2 Hz), 7.58 (d, 1H, ³J = 16.0 Hz); ¹³C NMR (100 MHz, CDCl₃): δ 13.6, 19.1, 30.7, 55.0, 64.0, 114.1, 115.5, 127.0, 129.5, 144.0, 161.2, 167.1.

2.5.7 (*E*)-1-Methoxy-4-styrylbenzene (**1g**)

¹H NMR (400 MHz, CDCl₃): δ 3.89 (s, 3H), 6.92 (d, 2H, ³J = 8.4 Hz), 6.99 (d, 2H, ³J = 16.4 Hz), 7.09 (d, 2H, ³J = 16.0 Hz), 7.36 (t, 2H, ³J = 7.6 Hz), 7.46–7.52 (m, 3H); ¹³C NMR (100 MHz, CDCl₃): δ 55.3, 114.1, 126.3, 126.6, 127.2, 127.8, 128.2, 128.7, 130.1, 137.7, 159.3.

2.5.8 (*E*)-*n*-Butyl 3-(4-chlorophenyl)acrylate (**1h**)

¹H NMR (400 MHz, CDCl₃): δ 0.90 (t, 3H, ³J = 7.2 Hz), 1.33–1.39 (m, 2H), 1.57–1.64 (m, 2H), 4.13 (t, 2H, ³J = 6.8 Hz), 6.64 (d, 1H, ³J = 16.0 Hz), 7.45 (d, 2H, ³J = 8.0 Hz), 7.63 (d, 1H, ³J = 16.0 Hz), 7.74 (d, 2H, ³J = 8.0 Hz); ¹³C NMR (100 MHz, CDCl₃): δ 13.7, 19.2, 30.7, 64.4, 118.8, 129.1, 129.4, 132.9, 136.0, 143.0, 166.7.

2.5.9 (*E*)-1-Chloro-4-styrylbenzene (**1i**)

¹H NMR (400 MHz, CDCl₃): δ 7.07 (s, 2H), 7.28–7.39 (m, 5H), 7.43–7.46 (m, 2H), 7.50–7.52 (m, 2H); ¹³C NMR (100 MHz, CDCl₃): δ 127.7, 128.5, 128.8, 129.0, 129.9, 130.0, 130.4, 134.3, 136.9, 138.1.

2.5.10 (*E*)-*n*-Butyl 3-(4-nitrophenyl)acrylate (**Ij**)

^1H NMR (400 MHz, CDCl_3): δ 0.92 (t, 3H, $^3J = 7.2$ Hz), 1.35–1.44 (m, 2H), 1.62–1.69 (m, 2H), 4.17–4.24 (m, 2H), 6.53 (d, 1H, $^3J = 16.0$ Hz), 7.63–7.68 (m, 3H), 8.20 (d, 2H, $^3J = 8.0$ Hz); ^{13}C NMR (100 MHz, CDCl_3): δ 13.6, 19.1, 30.6, 64.7, 122.5, 124.0, 128.6, 140.5, 141.5, 148.3, 166.0.

2.5.11 (*E*)-*n*-Butyl 3-(4-cyanophenyl)acrylate (**Ik**)

^1H NMR (400 MHz, CDCl_3): δ 0.77 (t, 3H, $^3J = 7.0$ Hz), 1.30–1.38 (m, 2H), 1.57–1.64 (m, 2H), 4.14 (t, 2H, $^3J = 6.8$ Hz), 6.45 (d, 1H, $^3J = 16.0$ Hz), 7.54 (d, 2H, $^3J = 8.4$ Hz), 7.57 (d, 1H, $^3J = 15.2$ Hz), 7.60 (d, 2H, $^3J = 8.0$ Hz); ^{13}C NMR (100 MHz, CDCl_3): δ 13.5, 19.0, 30.5, 64.4, 113.0, 118.1, 121.6, 128.3, 132.4, 138.4, 141.8, 165.7.

2.5.12 (*E*)-4-Styrylbenzotrile (**Il**)

^1H NMR (400 MHz, CDCl_3): δ 7.09 (d, 1H, $^3J = 16.0$ Hz), 7.22 (d, 1H, $^3J = 16.0$ Hz), 7.31–7.34 (t, 1H, $^3J = 4.0$ Hz), 7.38–7.41 (t, 2H, $^3J = 4.0$ Hz), 7.54 (d, 2H, $^3J = 7.2$ Hz), 7.58 (d, 2H, $^3J = 8.4$ Hz), 7.64 (d, 2H, $^3J = 8.4$ Hz); ^{13}C NMR (100 MHz, CDCl_3): δ 111.7, 120.2, 127.8, 128.0, 128.1, 129.8, 130.0, 133.5, 133.6, 137.4, 142.9.

2.5.13 (*E*)-1-Nitro-4-styrylbenzene (**Im**)

^1H NMR (400 MHz, CDCl_3): δ 7.06–7.18 (m, 1H), 7.40–7.45 (m, 4H), 7.49–7.66 (m, 4H), 8.15–8.26 (m, 2H); ^{13}C NMR (100 MHz, CDCl_3): δ 125.2, 127.4, 128.0, 128.2, 130.0, 134.4, 137.3, 145.0, 147.8.

2.6 General Procedure for Suzuki Coupling Reaction

A mixture of aryl halide (1 mmol), phenylboronic acid (1.5 mmol), Et_3N (2 mmol) and Pd-imino-Py- $\gamma\text{-Fe}_2\text{O}_3$ (0.25 mol%, 0.009 g) was stirred at 100 °C in DMF (2 mL) for an appropriate time (Table 3). The catalyst was separated by an external magnet, washed with EtOH, dried and reused for a consecutive run under the same reaction conditions. Evaporation of the solvent of the filtrate under reduced pressure gave the crude products. The pure products were isolated by chromatography on silica gel eluted with *n*-hexane:EtOAc (50:1).

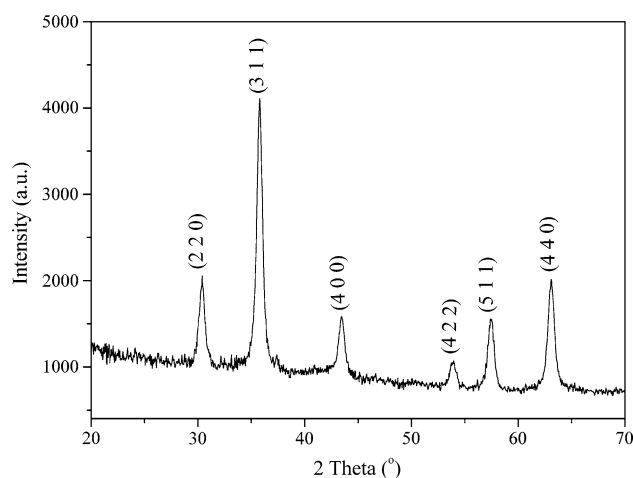
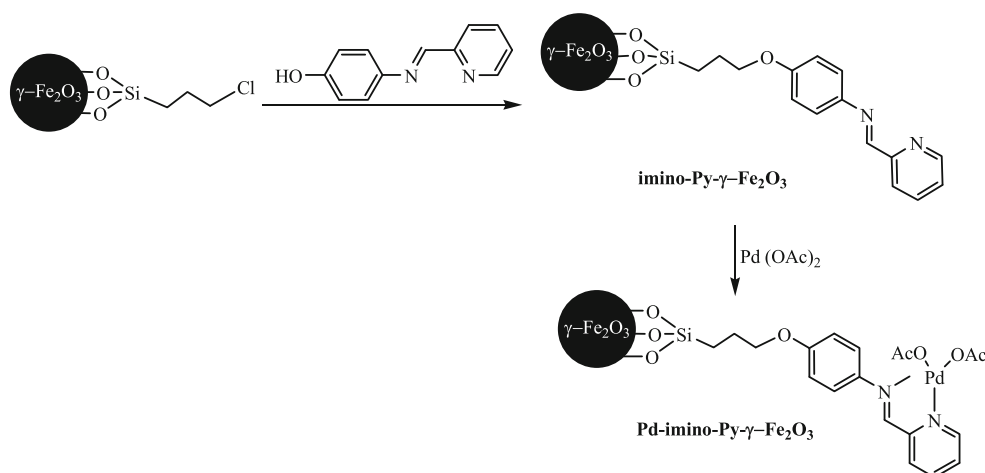


Fig. 1 XRD patterns of Pd-imino-Py- $\gamma\text{-Fe}_2\text{O}_3$



Scheme 1 Synthesis of Pd-imino-Py- $\gamma\text{-Fe}_2\text{O}_3$

Fig. 2 SEM of Pd-imino-Py- γ - Fe_2O_3

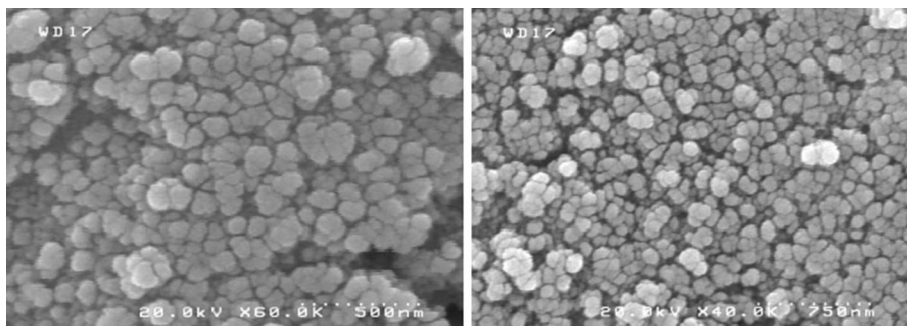


Fig. 3 a TEM of Pd-imino-Py- γ - Fe_2O_3 and **b** particle size distribution histogram of Pd-imino-Py- γ - Fe_2O_3

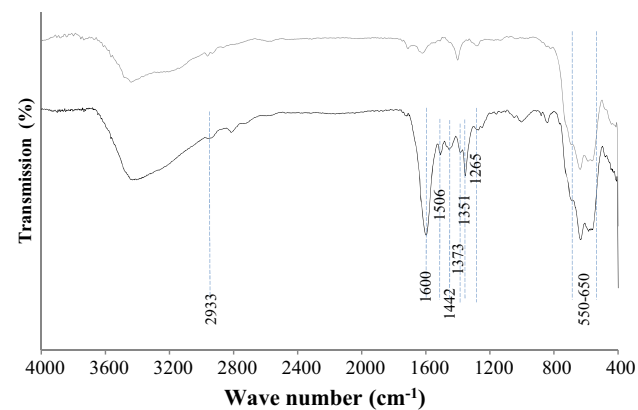
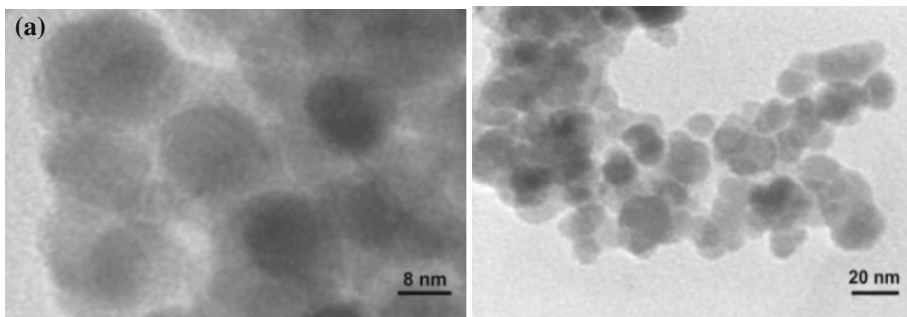


Fig. 4 FT-IR spectra of γ - Fe_2O_3 (gray), Pd-imino-Py- γ - Fe_2O_3 (black)

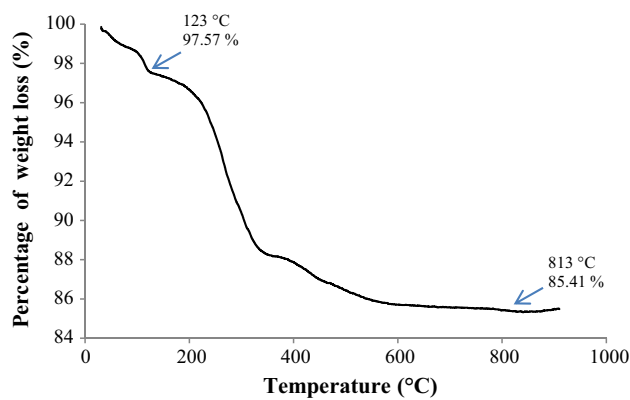


Fig. 5 TGA of Pd-imino-Py- γ - Fe_2O_3

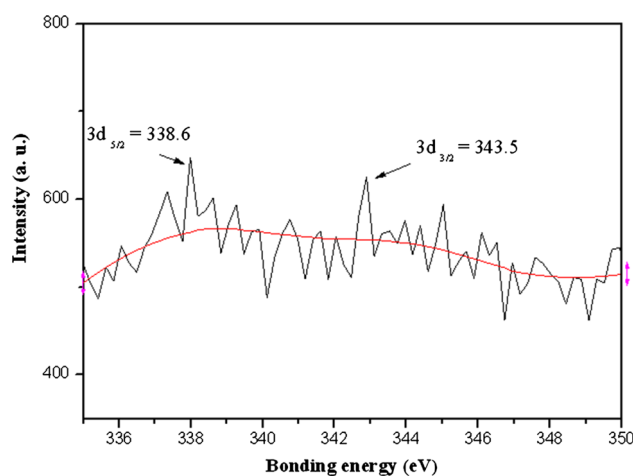


Fig. 6 XPS spectrum of Pd-imino-Py- γ -Fe₂O₃

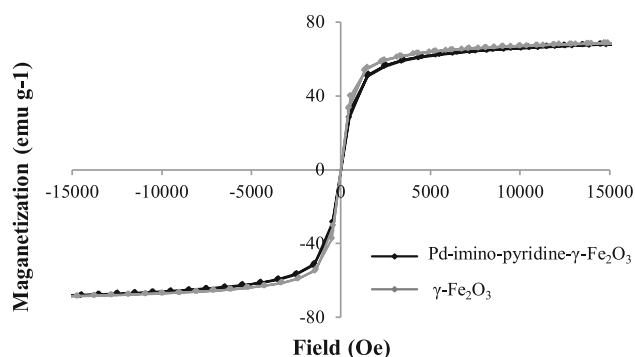


Fig. 7 Magnetization curves of γ -Fe₂O₃ and Pd-imino-Py- γ -Fe₂O₃

2.6.1 Biphenyl (2a)

¹H NMR (400 MHz, CDCl₃): δ 7.46 (t, 2H, ³J = 7.2 Hz), 7.56 (t, 4H, ³J = 8.0 Hz), 7.72 (d, 4H, ³J = 6.8 Hz); ¹³C NMR (100 MHz, CDCl₃): δ 127.2, 127.3, 128.8, 141.3.

2.6.2 4-Methoxybiphenyl (2b)

¹H NMR (400 MHz, CDCl₃): δ 3.83 (s, 3H), 6.99 (d, 2H, ³J = 8.8 Hz), 7.31 (t, 1H, ³J = 7.2 Hz), 7.43 (t, 2H, ³J = 8.0 Hz), 7.55 (t, 4H, ³J = 8.8 Hz); ¹³C NMR (100 MHz, CDCl₃): δ 56.5, 115.3, 127.8, 127.9, 129.3, 129.9, 134.9, 142.0, 160.3.

2.6.3 4-Nitrobiphenyl (2c)

¹H NMR (400 MHz, CDCl₃): δ 7.43–7.52 (m, 3H), 7.62–7.64 (m, 2H), 7.73–7.76 (m, 2H), 8.29–8.30 (m, 2H); ¹³C NMR (100 MHz, CDCl₃): δ 125.2, 128.5, 128.9, 130.0, 130.3, 139.9, 148.2, 148.7.

2.6.4 4-Cyanobiphenyl (2d)

¹H NMR (400 MHz, CDCl₃): δ 7.41–7.51 (m, 3H), 7.56–7.60 (m, 2H), 7.68–7.74 (m, 4H); ¹³C NMR (100 MHz, CDCl₃): δ 112.0, 120.1, 128.3, 128.8, 129.8, 130.2, 133.7, 140.3, 146.8.

3 Results and Discussion

3.1 Synthesis and Characterization of Pd-Imino-Py- γ -Fe₂O₃

Pd-imino-Py- γ -Fe₂O₃ was synthesized by the simple procedure shown in Scheme 1. At first, chloro-functionalized γ -Fe₂O₃ [34] was reacted with iminopyridine ligand to obtain Schiff base immobilized on γ -Fe₂O₃. Finally, the reaction of imino-Py- γ -Fe₂O₃ with Pd(OAc)₂ in dry acetone led to the formation of palladium-Schiff base complex supported on γ -Fe₂O₃ MNPs (Pd-imino-Py- γ -Fe₂O₃).

The synthesized catalyst was characterized by XRD (X-ray diffraction), SEM (scanning electron microscopy), TEM (high resolution transmission electron microscopy), FT-IR (Fourier transform infrared spectroscopy), TGA (thermogravimetric analysis), elemental analysis, ICP (inductively coupled plasma), elemental analysis, XPS (X-ray photoelectron spectroscopy) and VSM (vibrating sample magnetometer).

As presented in Fig. 1, the reflection planes of (2 2 0), (3 1 1), (4 0 0), (4 2 2), (5 1 1) and (4 4 0) at $2\theta = 30.3^\circ$, 35.7° , 43.4° , 53.8° , 57.4° and 63.0° were readily recognized from the XRD pattern of Pd-imino-Py- γ -Fe₂O₃. The observed diffraction peaks was indicated that γ -Fe₂O₃ magnetic nanoparticles mostly exist in face-centered cubic structure. The average crystallite size of Pd-imino-Py- γ -Fe₂O₃ (16 nm) was estimated using the Debye–Scherrer formula.

SEM images of Pd-imino-Py- γ -Fe₂O₃ were showed uniformity and spherical morphology of MNPs (Fig. 2).

As can be seen from the TEM images, imino-Py- γ -Fe₂O₃ has spherical morphology with relatively good monodispersity. The particle size distribution of Pd-imino-Py- γ -Fe₂O₃ was evaluated using TEM (Fig. 3). The average diameter of nanoparticles was 15 nm.

FT-IR spectra of γ -Fe₂O₃ and Pd-imino-Py- γ -Fe₂O₃ were shown in Fig. 4. The band at around $550\text{--}650\text{ cm}^{-1}$ was assigned to the stretching vibrations of Fe–O bond in γ -Fe₂O₃ and Pd-imino-Py- γ -Fe₂O₃. In the spectrum of Pd-imino-Py- γ -Fe₂O₃, the C–H stretching mode of methylene can be observed at 2933 cm^{-1} . Two absorption bands at 1506 and 1442 cm^{-1} was attributed to the stretching vibration of C=C bonds. The presence of bands at around

1351 and 1265 cm^{-1} was allocated to C-N and C-O stretching vibrations, respectively. Peaks were appeared at 1600 and 1373 cm^{-1} in the spectrum of Pd-imino-Py- γ - Fe_2O_3 , related to COO (in acetate) and confirmed the presence of Pd in the catalyst. These results indicated that Schiff base were successfully grafted onto the γ - Fe_2O_3 MNPs.

The thermogravimetric analysis (TGA) of Pd-imino-Py- γ - Fe_2O_3 was used to determine the thermal stability and content of organic functional groups on the surface of MNPs (Fig. 5). TG curve of Pd-imino-Py- γ - Fe_2O_3 showed the weight loss around 110 $^\circ\text{C}$, which was related to the adsorbed water molecules on the support. The organic parts were decomposed completely in the temperature range of 123–813 $^\circ\text{C}$. According to the TGA, the amount of components supported on γ - Fe_2O_3 is estimated to be 0.26 mmol g^{-1} . These results were in good agreement with the elemental analysis data ($N = 0.75\%$ and $C = 6.25\%$) and ICP. The ICP analysis showed that 0.26 mmol of Pd(II) was anchored on 1.0 g of MNPs [Pd(II) wt% = 2.8 %].

In the X-ray photoelectron spectrum (XPS) of Pd-imino-Py- γ - Fe_2O_3 , binding energies at 338.6 and 343.5 eV corresponding to Pd 3d_{5/2} and Pd 3d_{3/2}, respectively, confirmed the presence of Pd(II) in the catalyst (Fig. 6).

The magnetization curves of γ - Fe_2O_3 and Pd-imino-Py- γ - Fe_2O_3 were measured at room temperature using a vibrating sample magnetometer (VSM). No reduced remanence and coercivity were detected, indicating both unmodified and Pd-imino-Py- γ - Fe_2O_3 are superparamagnetic (Fig. 7). The value of saturation magnetic moments of γ - Fe_2O_3 and Pd-imino-Py- γ - Fe_2O_3 are 68.9 emu g^{-1} .

3.2 Catalytic Activity of Pd-Imino-Py- γ - Fe_2O_3 in Heck and Suzuki Cross-Coupling Reactions

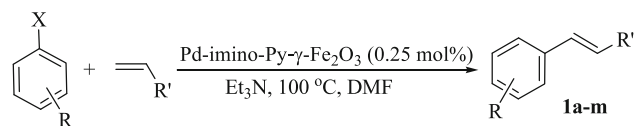
Following the successful synthesis of Pd-imino-Py- γ - Fe_2O_3 , its effectiveness for Heck and Suzuki cross-coupling reactions were examined. At first, Heck cross-coupling reaction of iodobenzene with *n*-butyl acrylate in the presence of 0.25 mol% of Pd-imino-Py- γ - Fe_2O_3 and Et₃N as a base was chosen as a model reaction (Table 1). This reaction was investigated under solvent-free conditions and in different solvents such as DMF, CH₃CN, toluene, EtOH and H₂O (Table 1, entries 1–6). The best yield of the desired product was obtained in DMF at 100 $^\circ\text{C}$ (Table 1, entry 2). A similar reaction at lower temperatures required longer reaction time and produced the desired product in lower yields (Table 1, entries 7 and 8). Increasing the reaction temperature to 120 $^\circ\text{C}$ did not have any significant

Table 1 Heck coupling reaction of iodobenzene with *n*-butyl acrylate under different conditions

Entry	Catalyst (mol%)	Solvent	Tem. ($^\circ\text{C}$)	Base	Time (h)	Yield ^a (%)
1	Pd-imino-Py- γ - Fe_2O_3 (0.25)	–	100	Et ₃ N	1.5	90
2	Pd-imino-Py- γ - Fe_2O_3 (0.25)	DMF	100	Et ₃ N	0.5	95
3	Pd-imino-Py- γ - Fe_2O_3 (0.25)	CH ₃ CN	reflux	Et ₃ N	1	46
4	Pd-imino-Py- γ - Fe_2O_3 (0.25)	Toluene	100	Et ₃ N	0.5	16
5	Pd-imino-Py- γ - Fe_2O_3 (0.25)	EtOH	reflux	Et ₃ N	0.5	55
6	Pd-imino-Py- γ - Fe_2O_3 (0.25)	H ₂ O	100	Et ₃ N	24	15
7	Pd-imino-Py- γ - Fe_2O_3 (0.25)	DMF	rt	Et ₃ N	24	21
8	Pd-imino-Py- γ - Fe_2O_3 (0.25)	DMF	80	Et ₃ N	1	80
9	Pd-imino-Py- γ - Fe_2O_3 (0.25)	DMF	120	Et ₃ N	0.5	96
10	Pd-imino-Py- γ - Fe_2O_3 (0.25)	DMF	100	K ₂ CO ₃	1.5	67
11	Pd-imino-Py- γ - Fe_2O_3 (0.25)	DMF	100	Na ₂ CO ₃	3	51
12	Pd-imino-Py- γ - Fe_2O_3 (0.25)	DMF	100	NaOAc	1.5	63
13	Pd-imino-Py- γ - Fe_2O_3 (0.25)	DMF	100	KOH	2	44
14	Pd-imino-Py- γ - Fe_2O_3 (0.25)	DMF	100	–	24	Trace
15	Pd-imino-Py- γ - Fe_2O_3 (0.12)	DMF	100	Et ₃ N	0.5	78
16	Pd-imino-Py- γ - Fe_2O_3 (0.2)	DMF	100	Et ₃ N	0.5	81
17	Pd-imino-Py- γ - Fe_2O_3 (0.5)	DMF	100	Et ₃ N	0.5	96
18	Pd-imino-Py- γ - Fe_2O_3 (1)	DMF	100	Et ₃ N	0.5	97
19	–	DMF	100	Et ₃ N	24	Trace
20	Pd(OAc) ₂ (0.25)	DMF	100	Et ₃ N	24	30

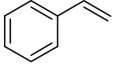
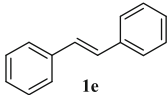
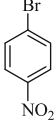
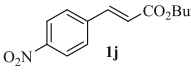
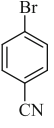
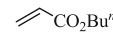
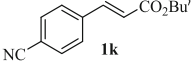
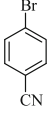
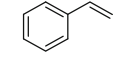
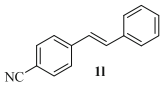
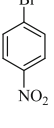
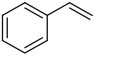
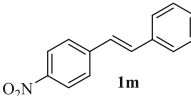
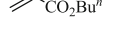
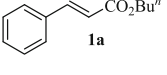
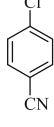
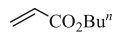
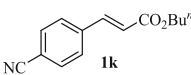
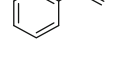
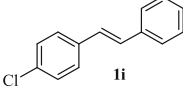
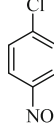
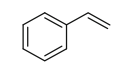
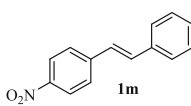
Reaction conditions iodobenzene:*n*-butyl acrylate:base = 1:1.5:2

^a Isolated yield

Table 2 Heck coupling reaction of various aryl halides with olefins catalyzed by Pd-imino-Py- γ -Fe₂O₃

Entry	Aryl halide	Olefin	Product	Time (h)	Yield ^a (%)
1				0.5	95
2				0.5	96
3				0.5	95
4				0.5	92
5				2	86
6				1	91
7				1.5	89
8				1.5	87
9				2.5	83
10				0.5	91

Table 2 continued

Entry	Aryl halide	Olefin	Product	Time (h)	Yield ^a (%)
11				2	94
12				0.5	93
13				0.5	92
14				2	87
15				2	89
16				4	92
17				4.5	85
18				5	86
19				5	88

Reaction conditions molar ratio of aryl halide:olefin:Et₃N:catalyst = 1:1.5:2:0.0025, 100 °C, DMF

^a Isolated yield. *Trans* isomer was obtained based on ³J_{HH} value (16.0–16.4 Hz) in the ¹H NMR spectra of the products

effect on the progress of the reaction (Table 1, entry 9). The influence of different bases on the reaction of iodobenzene with *n*-butyl acrylate in DMF at 100 °C was studied (Table 1, entries 10–13). Comparison of the results with those obtained in the presence of Et₃N showed that Et₃N was the best choice among the examined bases

(Table 1, entry 2). It is worth to note that the reaction did not proceed well in the absence of the base and only a trace amount of the desired product was formed after 24 h (Table 1, entry 14). Similar reactions were also performed in the presence of different catalytic amounts of Pd-imino-Py-γ-Fe₂O₃ (Table 1, entries 15–18) and found that

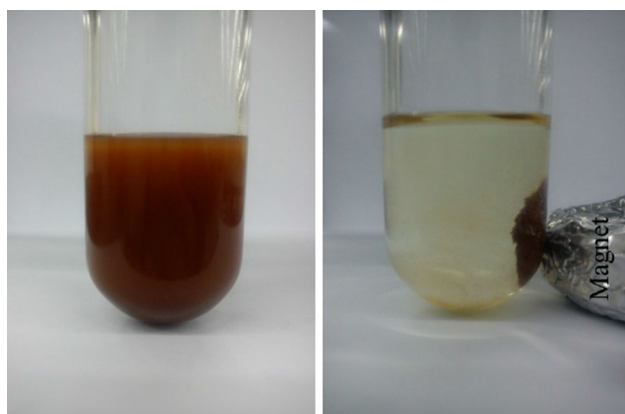


Fig. 8 Catalyst separation from the reaction mixture using an external magnet

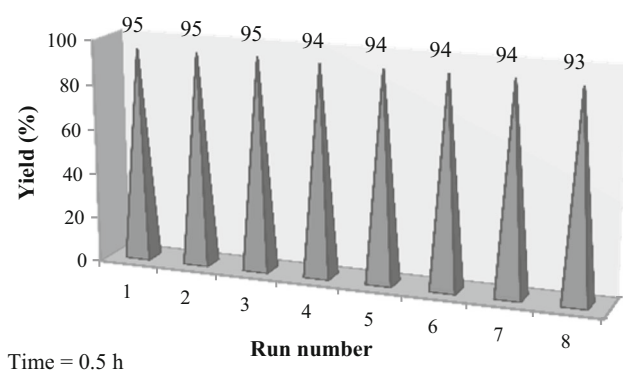


Fig. 9 Reusability of Pd-imino-Py- γ -Fe₂O₃ for the synthesis of *n*-butyl cinnamate (**1a**)

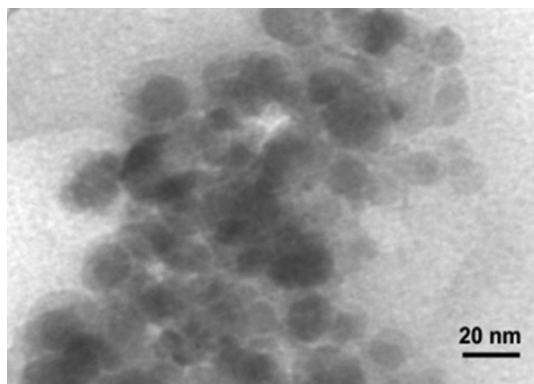


Fig. 10 TEM image of Pd-imino-Py- γ -Fe₂O₃ after eight times reuse 0.25 mol % of the catalyst, which was used in the model reaction was the best amount (Table 1, entry 2). The model reaction was examined in the absence of the catalyst and in the presence of Pd(OAc)₂ (Table 1, entries 19 and 20) and low amounts of the desired product were obtained after 24 h.

In order to establish the generality of this method, the Heck coupling reaction of a variety of aryl halides with

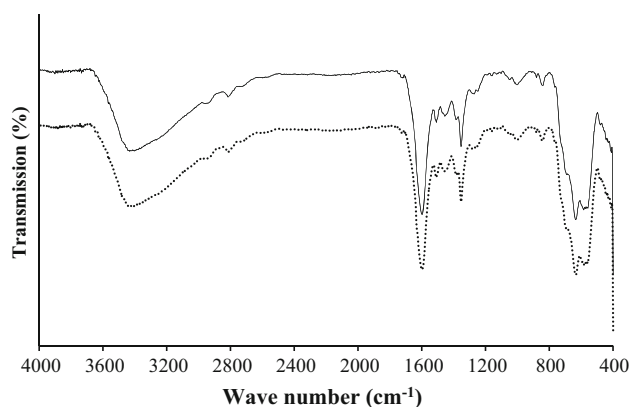
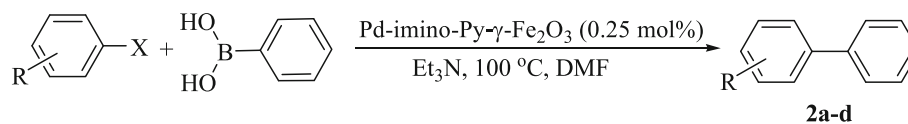


Fig. 11 FT-IR spectra of recovered Pd-imino-Py- γ -Fe₂O₃ (dotted line) and fresh Pd-imino-Py- γ -Fe₂O₃ (continuous line)

olefins under optimized reaction conditions (Table 1, entry 2) was investigated (Table 2).

As shown in Table 2, Pd-imino-Py- γ -Fe₂O₃ was effective for coupling reactions of iodobenzene with various olefins to give the corresponding products in 86–96 % (Table 2, entries 1–5). It was observed that iodobenzene functionalized with electron-withdrawing or electron-donating groups reacted with olefins and generated the corresponding products in good to high yields (Table 2, entries 6–9). This catalytic system was also successfully applied for the coupling reaction of substituted aryl bromides with various olefins (Table 2, entries 10–15). Although aryl chlorides are not as reactive and are less commonly employed in palladium-catalyzed coupling reactions, Heck reaction of aryl chlorides with olefins was successfully performed in the presence of Pd-imino-Py- γ -Fe₂O₃ and the desired products were produced in good to high yield (Table 2, entries 16–19).

The possibility of leaching of active species from the catalyst into the reaction mixture is known as a key factor of the catalyst stability. To investigate the extent of Pd leaching from Pd-imino-Py- γ -Fe₂O₃, the Heck cross-coupling reaction of iodobenzene with *n*-butyl acrylate was carried out in the presence of 0.25 mol % of the catalyst at 100 °C. The supported catalyst was filtered off after 50 % of the Heck reaction was proceeded and the filtrate was allowed to react further. The catalyst filtration was performed at the reaction temperature (100 °C) in order to avoid possible recoordination or precipitation of soluble Pd upon cooling. The result showed that after this hot filtration, further reaction was not observed. ICP analysis of the remaining solution revealed that there was no Pd in the reaction mixture. These results confirmed that the supported palladium MNPs was stable and could tolerate the present reaction conditions without leaching of the significant quantity of Pd.

Table 3 Suzuki coupling reaction of various aryl halides with phenylboronic acid catalyzed by Pd-imino-Py- γ -Fe₂O₃

Entry	Aryl halide	Product	Time (h)	Yield ^a (%)
1			0.5	95
2			1	92
3			1.5	86
4			2.5	91
5			3	85
6			2.5	94
7			2.5	87
8			5	91
9			4.5	90
10			4.5	86

Reaction conditions molar ratio of aryl halide:phenylboronic acid:Et₃N:catalyst = 1:1.5:2:0.0025, 100 °C, DMF

^a Isolated yield

Table 4 Catalytic activity of Pd-imino-Py- γ -Fe₂O₃ in comparison with other supported Pd catalysts on MNPs used for Heck and Suzuki cross-coupling reactions

Entry	Reaction	Catalyst (mol%) [Ref]	Tem. (°C)	Ar-X	Time (h)	Yield (%) ^a	TON ^b	TOF ^c (h ⁻¹)
1	Heck	Pd(0)-ZnFe ₂ O ₄ (4.62) [43]	78	I	2–14	80–96 ^d	17–21	1–10
				Br	6–12	65–90	14–19	1–3
2	Heck	Pd(0)-NH ₂ -Fe ₃ O ₄ (5) [44]	130	I	10	99 ^d	20	2
				Br	10–24	93–99 ^d	19–20	1–2
3	Heck	Pd(0)-Fe ₃ O ₄ @C (0.308) [45]	120	I	1–4	66–100	11–16.7	4.2–16.7
				Br	2–4	65–98	11–16.3	3.6–8.1
				Cl	4–10	4.3–58	0.7–9.8	0.18–0.98
4	Heck	Pd(II)-phosphine-Fe ₃ O ₄ @SiO ₂ (1) [46]	100	I	8	88–98	88–98	11–12.2
				Br	8	51–90	51–90	6.4–11.2
5	Heck	Pd(II)-isatin- γ -Fe ₂ O ₃ (0.5 and 1.5) [38]	100	I	0.5–4	87–95	174–190	43.5–380
				Br	2–7	63–90	51–128	12–28
				Cl	0.5–6	60–90	40–60	8–120
6	Heck	Pd(II)-DABCO ^e - γ -Fe ₂ O ₃ (1 and 3) [35]	100	I	0.5–6	73–92	24–92	2–184
				Br	3–8	61–84	20–84	2.5–28
				Cl	10–24	43–63	14–21	0.7–2
7	Heck	Pd(II)-acetamidine- γ -Fe ₂ O ₃ (0.12) [40]	100	I	0.5–3	79–96	658–800	233–1600
				Br	0.5–6	13–70	108–583	22–1150
				Cl	9	41	342	38
8	Heck	Pd(II)-BIP ^f -SiO ₂ @ γ -Fe ₂ O ₃ (0.5) [41]	100	I	0.25–3	80–98	160–196	53–784
				Br	2.5–4	82–92	164–184	46–74
				Cl	5–7	75–91	150–182	21–33
9	Heck	Pd(II)-imino-Py- γ -Fe ₂ O ₃ (0.25) ^{this work}	100	I	0.5–2.5	83–96	332–384	133–768
				Br	0.5–2	87–94	348–376	174–744
				Cl	4–5	85–92	340–368	69–92
10	Suzuki	Pd(II)-salen-SiO ₂ @Fe ₃ O ₄ (0.5) [47]	100–130	I	1	94–100	188–200	188–200
				Br	3	85–100	170–200	57–67
				Cl	6	11–43	22–86	4–14
11	Suzuki	Pd(0)-ZnFe ₂ O ₄ (4.62) [43]	78	I	3–8	90–95 ^d	19–20	6–7
				Br	3.5–9	85–91 ^d	18–20	2–6
12	Suzuki	Pd(0)-Fe ₃ O ₄ @C (0.308) [45]	78–153	I	1–2	72.3–100	12–16.2	8.1–16.7
				Br	1–3	54–98	9–16.3	4.6–16.3
				Cl	1–5	6–95	1–15.8	1–4
13	Suzuki	Pd(II)-phosphine-Fe ₃ O ₄ @SiO ₂ (0.5) [46]	60	I	1.5	90–99	180–198	120–132
				Br	10	26–52	52–104	5.2–10.4
14	Suzuki	Pd(II)-isatin- γ -Fe ₂ O ₃ (0.5 and 1.5) [38]	100	I	0.5–3	83–95	166–190	62–380
				Br	3/4–4.5	60–97	47–194	43–80
				Cl	1–1.5	76–93	51–62	13–62
15	Suzuki	Pd(II)-acetamidine- γ -Fe ₂ O ₃ (0.12) [40]	100	I	0.5–2	63–96	525–800	262–1600
				Br	0.5–2	81–96	675–800	337–1600
				Cl	5–10	41–50	342–417	34–75
16	Suzuki	Pd(II)-BIP ^f -SiO ₂ @ γ -Fe ₂ O ₃ (0.5) [41]	100	I	1–2	90–98	180–196	90–196
				Br	2.5–3	91–92	182–184	61–74
				Cl	4–5	82–86	164–172	33–43

Table 4 continued

Entry	Reaction	Catalyst (mol%) [Ref]	Tem. (°C)	Ar-X	Time (h)	Yield (%) ^a	TON ^b	TOF ^c (h ⁻¹)
17	Suzuki	Pd(II)-imino-Py- γ -Fe ₂ O ₃ (0.25) [this work]	100	I	0.5–1.5	86–95	344–380	229–760
				Br	2.5–3	85–94	340–376	113–150
				Cl	4.5–5	86–91	344–364	76–80

^a Isolated yield^b TON = turnover number (ratio of moles of product formed to moles of catalyst)^c TOF = turnover frequency (TON per hour)^d Determined by GC^e DABCO: 1,4-diazabicyclo[2.2.2]octane^f BIP: bis(imino)pyridine

For practical applications of a heterogeneous catalyst, reusability of the catalyst is a very significant factor [42]. To clarify this issue, catalytic recycling experiments were carried out using Heck cross-coupling reaction of iodobenzene with *n*-butyl acrylate under optimized reaction conditions. After the reaction was completed, it was cooled to room temperature and the whole amount of Pd-imino-Py- γ -Fe₂O₃ simply was separated from the product by an external magnet (Fig. 8).

The recovered catalyst was washed with EtOH, dried at room temperature and reused for a similar reaction. It was found that Pd-imino-Py- γ -Fe₂O₃ could be recycled and reused for eight consecutive trials without loss of its catalytic activity (Fig. 9).

ICP and elemental analyses ($N = 0.75\%$ and $C = 6.25\%$) of Pd-imino-Py- γ -Fe₂O₃ after eight reuses showed that only a very small amount ($<1\%$) of Pd was removed from the catalyst. Comparison of TEM image (Fig. 10) and FT-IR spectrum of used catalyst (Fig. 11) with one of the fresh catalyst (Fig. 3) showed that the morphology and structure of Pd-imino-Py- γ -Fe₂O₃ remained intact after eight recoveries.

Encouraged by the satisfactory results with the Heck cross-coupling reaction, the Pd-imino-Py- γ -Fe₂O₃ catalyst was applied to the Suzuki coupling reaction (Table 3).

As the results of Table 3 indicate, the electron-neutral, electron-rich and electron-poor iodobenzenes reacted with phenylboronic acid to generate the Suzuki cross-coupling products in 86–95% (Table 3, entries 1–3). This method was also applicable for the cross-coupling reaction of differently substituted bromobenzenes and chlorobenzenes with phenylboronic acid (Table 3, entries 4–10).

A comparison of the activity of various immobilized palladium catalysts with Pd-imino-Py- γ -Fe₂O₃ in the Heck and Suzuki coupling reactions published in the literature is listed in Table 4.

Catalytic activity of Pd-imino-Py- γ -Fe₂O₃ was compared with other palladium catalysts supported on MNPs

for the Heck and Suzuki cross-coupling reactions (Table 4). It is appeared that Pd-imino-Py- γ -Fe₂O₃ showed good catalytic activity, but comparing with the others the advantage is not remarkable, even some catalytic systems are much better than ours for coupling reaction of aryl iodides or bromides. More importantly, the procedure followed by us provides significant advantages in terms of TON and TOF compared with the other catalytic systems toward aryl chlorides as challenging substrates.

4 Conclusions

In conclusion, a novel covalently immobilized palladium-Schiff base complex on magnetic nanoparticles (Pd-imino-Py- γ -Fe₂O₃) has been synthesized and characterized by different techniques. Pd-imino-Py- γ -Fe₂O₃ not only exhibits an impressive catalytic activity in Heck and Suzuki cross-coupling reactions, but also possesses high stability. As magnetic nanoparticles were used as the solid support, the present catalyst was simply separated from the reaction mixture by an external magnet, and reused at least for eight consecutive runs without Pd leaching and significant loss of its catalytic activity. The merits associated with Pd-imino-Py- γ -Fe₂O₃ hopefully will render it a valuable catalyst in practical synthesis.

Acknowledgments We are thankful to University of Birjand Research Council for their support on this work.

References

- Meijere A, Brase S, Oesterich M (2014) Metal-catalyzed cross-coupling reactions and more. Wiley, Weinheim
- Beller M, Bolm C (2004) Transition metals for organic synthesis, 2nd edn. Wiley, Weinheim
- Torborg C, Beller M (2009) Adv Synth Catal 351:3027
- Vries JG (2001) Can J Chem 79:1086

5. Cho JH, Shaughnessy KH (2011) *Synlett* 2963
6. Suzuki A (2003) In: Astruc D (ed) *Modern arene chemistry*. Wiley, Weinheim, pp 53–106
7. Xi CJ, Wu YW, Yan XY (2008) *J Organomet Chem* 693:3842
8. Kawano T, Shinomaru T, Ueda I (2002) *Org Lett* 4:2545
9. Herrmann WA, Reisinger CP, Spiegler M (1998) *J Organomet Chem* 557:93
10. Amatore C, Jutand A (1998) *Coord Chem Rev* 178:511
11. Baleizao C, Corma A, Garcia H, Leyva A (2004) *J Org Chem* 69:439
12. Feng XJ, Yan M, Zhang T, Liu Y, Bao M (2010) *Green Chem* 12:1758
13. Zhang J, Zhao GF, Popovic Z, Lu Y, Liu Y (2010) *Mater Res Bull* 45:1648
14. Ali H, Cauchon N, Lier JEV (2009) *Photochem Photobiol Sci* 8:868
15. Lai YC, Chen HY, Hung WC, Lin CC, Hong FE (2005) *Tetrahedron* 61:9484
16. Mehendale NC, Sietsma JRA, Jong KPD, Walree CAV, Gebbink RJMK, Koten GV (2007) *Adv Synth Catal* 349:2619
17. Molnar A (2011) *Chem Rev* 111:2251
18. Koukabi N, Kolvari E, Zolfigol MA, Khazaei A, Shirmardi Shaghasemi B, Fasahati B (2012) *Adv Synth Catal* 354:2001
19. Dyal A, Loos K, Noto M, Chang SW, Spagnoli C, Shafi KVPM, Ulman A, Cowman M, Gross RA (2003) *J Am Chem Soc* 125:1684
20. Rafiee E, Eavani S (2011) *Green Chem* 13:2116
21. Liu YH, Deng J, Gao JW, Zhang ZH (2012) *Adv Synth Catal* 354:441
22. Esmailpour M, Sardarian AR, Javidi J (2014) *J Organomet Chem* 749:233
23. Beygzadeh M, Alizadeh A, Khodaei MM, Kordestani D (2013) *Catal Commun* 32:86
24. Karimi B, Mansouri F, Mirzaei HM (2015) *ChemCatChem* 7:1736
25. Dileep R, Badekai RB (2010) *Appl Organometal Chem* 24:663
26. Ballus KJ, Khanmamedova AK, Dixon KM, Bedioui F (1996) *Appl Catal A* 143:159
27. Heinrichs C, Holderich WF (1999) *Catal Lett* 58:75
28. Sobhani S, Pakdin Parizi Z, Razavi N (2011) *Appl Catal A* 409–410:162
29. Sobhani S, Pakdin Parizi Z, Nasserri R (2013) *J Chem Sci* 125:975
30. Sobhani S, Jahanshahi R (2013) *New J Chem* 37:1009
31. Sobhani S, Bazrafshan M, Arabshahi Delluei A, Pakdin Parizi Z (2013) *Appl Catal A* 454:145
32. Sobhani S, Honarmand M (2013) *Appl Catal A* 467:456
33. Sobhani S, Pakdin Parizi Z (2014) *RSC Adv* 4:13071
34. Sobhani S, Mesbah Falatoooni Z, Honarmand M (2014) *RSC Adv* 4:15797
35. Sobhani S, Pakdin Parizi Z (2014) *Appl Catal A* 479:112
36. Sobhani S, Honarmand M (2013) *Catal Lett* 143:476
37. Sobhani S, Ghasemzadeh MS, Honarmand M (2014) *Catal Lett* 144:1515
38. Sobhani S, Zarifi F (2015) *Chin J Catal* 36:555
39. Sobhani S, Vahidi Z, Zeraatkar Z, Khodadadi S (2015) *RSC Adv* 5:36552
40. Sobhani S, Ghasemzadeh MS, Honarmand M, Zarifi F (2014) *RSC Adv* 4:44166
41. Sobhani S, Zeraatkar Z, Zarifi F (2015) *New J Chem* 39:7075
42. Molnar A (2011) *Chem Rev* 111:2251
43. Singh AS, Patil UB, Nagarkar JM (2013) *Catal Commun* 35:11
44. Zhang F, Jin J, Zhong X, Li S, Niu J, Li R, Ma J (2011) *Green Chem* 13:1238
45. Zhu M, Diao G (2011) *J Phys Chem C* 115:24743
46. Li P, Wang L, Zhang L, Wang GW (2012) *Adv Synth Catal* 354:1307
47. Jin X, Zhang K, Sun J, Wang J, Dong Z, Li R (2012) *Catal Commun* 26:199